Influence of Moisture on Shape Memory and Mechanical Properties of Microwave-induced Shape Memory Polyurethane (PU)/graphene Nanoplatelets (GNPs) Composite

KRISHAN KUMAR PATEL[1*], RAJESH PUROHIT[1], S.A.R. HASHMI[2], AND RITESH KUMAR GUPTA[2]

[1]Mechanical Engineering Department, Maulana Azad National Institute of Technology Bhopal, 462003 India.
[2]Polymer composite lab, Advanced Materials and Processes Research Institute (CSIR-AMPRI) Bhopal, 462024 India.

ABSTRACT

Microwave-induced shape memory polymer (Polyurethane)/Graphene nanoplatelets composite were prepared in micro-compounder. When samples exposed in moisture (immersed in water), the thermo-mechanical and shape memory properties such as Tensile strength, glass transition temperature, storage modulus, stretch and recovery strength were decreased. The surface morphology and dispersion of GNPs in PU matrix were characterized by using the Atomic Force Microscopy (AFM), X-ray Diffraction (XRD) and Field Emission Scanning Electron Microscopy (FE-SEM). Further, we found that the PU specimen has no shape recovery during MV irradiations without moisture exposed sample. But moisture exposed PU sample shows shape recovery. With increasing water immersion time (Days) of the PU and 1 GPU samples the MV-induced shape recovery was increased. Because the absorbed water molecules in samples act as a dielectric note heating source for MV irradiations. So that its novel approach which may treat as a self-responsive shape memory polymer components when exposed long days in moisture.

KEY WORDS : *Shape memory polymer, Microwave, Moisture, GNPs, Glass transition temperature.*

J. Polym. Mater. Vol. **35,** No. 4, 2018, 449-462

Correspondence author e-mail: krishan.patel4@gmail.com
DOI : https://doi.org/10.32381/JPM.2018.35.04.4

1. INTRODUCTION

Shape memory polymers are a smart, intellectually, functionally graded, self-healing, lightweight, low cost, ease of fabrication as compared to existing shape memory alloys and shape memory ceramics [1-5]. As a exploring new research in science and technology day by day, the shape memory polymer nano-composite components takes place over the existing components [2,6,7]. Shape memory polymers (SMPs) usually used for various applications such as sensors and actuators, remote sensing and wireless, bio-medical devices, robotics and other sophisticated applications. Shape memory materials are the class of self actuating materials which are switching the one temporary shape to other permanent shape with the help of number of external stimuli such as, temperature [3], magnetic field [8], electric current, ph [6-7], water [9], solutions, electromagnetic rays[10], microwave etc [11]. The polyurethane-based shape memory polymer may categorise into two parts one is thermosetting polyurethane and thermoplastic polyurethane [12-16]. The thermosetting polyurethane has also two parts one is reign and another is hardener. The thermosetting polymer samples directly made by the solvent casting method whereas thermoplastic polyurethane based samples were prepared by melt mixing route [17-25]. The shape memory polymer (SMPs) has several disadvantages like low recovery stress, low glass transition temperature, low strength easily affected by moisture [11]. So that for overcome such disadvantages the shape memory polymer composites were introduced by reinforcing the various reinforcement such as TiC, SiC. CNTs, GNPs and Fibre etc [26-34, 12]. Thermo-responsive [24], Ph-responsive [6, 9], light responsive [23], electric responsive [25, 26], magnetic responsive [2, 12] and water responsive [34] shape memory polymers have a traditional (conventional) method to triggered the shape memory polymer components. Various researchers already reported that the improved shape memory and mechanical properties of light responsive [23, 29], Microwave responsive [13, 14, 28], electromagnetic responsive shape memory polymer composites. But when we think about the non-traditional, non-contact, clean green stimuli for shape recovery we go for Electromagnetic responsive, Microwave responsive and moisture responsive shape memory polymer composites [23, 25, 33-42]. From the literature survey, we observed that many researchers are working in thermo-responsive and other conventionally triggered shape memory polymer composites [11, 13, 24]. Recently few researchers started working on microwave and moisture responsive shape memory polymer composites [35-37]. Microwave [38] and moisture [36] responsive shape memory polymer have a clean green and non-contact source for shape recovery which is widely useful for wireless, remote sensing and other sophisticated applications [39-44].

In our research paper, the effect of moisture on Microwave-induced thermoplastic shape memory polyurethane (PU)/ graphene nanoplatelets composite were studied. The pure and composite containing 1 phr GNPs in the PU matrix (namely 1 GPU) were prepared through melt mixing rout in micro-compounder. The PU and 1 GPU samples were immersed in a water bath for 5 days and 10 days for testing and characterizations. The tensile strength, glass transition temperature, stretch and

recovery strength were decreased due to the moisture. Dynamic Mechanical Analyser (DMA) was used to study the thermo-mechanical properties of viscoelastic materials. The glass transition temperature was calculated by using the DMA and DSC curves. On another hand the due to the moisture, microwave-induced shape recovery was improved for both Pure and composite sample. Pure PU sample without water immersed has no shape recovery but when PU sample immersed in water than after its shows MV-induced shape recovery. Further, we concluded that the moisture responsive shape memory polymer can play an important role in various wireless, non-contact heating, sensors and actuators.

2. THE MATERIAL, SAMPLE PREPARATION AND CHARACTERIZATIONS

2.1 Material

Shape memory thermoplastic polyurethane (PU) ether type granules MM6520 was purchased from Mitsubishi (diplex) Japan supplied by Nano Shel Pvt. Ltd. graphene nanoplatelets (GNPs) having 11-15 nm obtained in powder form from Lo-Li Tech. GmbH nonmaterial's Germany.

2.2 Sample preparations

In sample preparation, the PU pallets and GNPs were dried at 110 °C for 5 hours in a vacuum oven to reduce the impurities. After that, the micro compounder and injection moulding were used to making samples of PU and 1 GPU (1 phr GNPs in PU matrix) composite. The preparation of sample procedure like same as reported [38]. 6g PU was taken and proceed in micro compounder followed by injection moulding. Thermo Haake micro-compounder MiniLab 3 and Thermo Scientific Haake Mini-jet pro Piston injection moulding were used. The speed of twin conical screw (micro-compounder) 60 rpm for 10 minutes and mixing temperature was 210°C. The injection pressure, post pressure, cylinder temperature, mould temperature, the injection time of injection moulding was 620 bar, 600 bar, 210°C, 85°C and 20 seconds respectively. Thereafter samples remove after 5 minutes from ISI slandered die (injection moulding ISI standard die) for testing and characterizations.

2.3 Scanning Electron Microscopy

Surface morphology studies were carried out by using the Scanning Electron Microscopy (SEM). The cryogenic fracture surfaces were observed in SEM after 100 A gold coating layer in samples for clear observations.

The shape memory test (stretch and recovery) was tested in the tensile testing machine (Tinius Olsen 25kt) for the standard tensile sample. The sample was clamped in spring-loaded grips and furnace start for heating the sample at 65°C. Once the sample temperate reached 65°C the test start to Appling the tensile strength upto 50% strain after that furnace was open to cool down the sample below 32°C without releasing the load. Once the sample temperature comes below 32°C sample open from the spring-loaded grip and final gauge length was a measure for shape fixity. Than after stretched sample again clamp in grips for measuring the recovery strength. The stretched sample clamp in grips and furnace closed to heat sample 65°C. Once the temperature of the sample reached 65°C the test was started to record the recovery stress. The same procedure was carried out for all samples. Details procedure we also discussed in the results and discussion section.

2.4 Uni-axial tensile testing

Tensile strength was also carried out for standard ISI tensile sample by using the Tinius Olsen25kt tensile testing machine at room temperature. The cross-head speed was 10mm/minutes.

2.5 Differential Scanning Calorimetric (DSC)

Differential Scanning Calorimetric (DSC) test was conducted by using DSC 1 STAR System M/s Mettler Toledo. The DSC heating results ranging from 25°C to 70°C were analysed in the discussion section. The glass transition temperature (Tg) was calculated by DSC curves.

2.6 Dynamic Mechanical Analyser (DMA)

Dynamic Mechanical Analyser (DMA) was used for calculation of thermo-mechanical properties of the viscoelastic material. The DMS 6100 Dynamic Mechanical Analyser by Hitachi instrument was used. The injection moulded sample 40x10x1 mm^3 was used in 3 points bending mode in the temperature range from 30°C to 80°C having 1Hz bending frequency. The DMA was used to determine the response of visco-elastic materials by application of dynamic load and temperature. The storage modulus, loss modulus and energy dissipation factor and glass transition temperature (Tan D) curves were analysed by using DMA.

2.7 Microwave-induced shape recovery tests

Microwave-induced shape recovery test was conducted by using the household microwave oven model (IFB 30SC3) supplied by Technical System Pvt, Ltd. The microwave oven having fixed power supplied 120W and frequency of 2.45 GHz and the distance between the two permatron was 30cm. before testing the MV-induced shape recovery the samples temporary deformed straight shape from original spring shape.

2.8 XRD analysis

X-Ray Diffraction (XRD) analysis was done by using XRD 6000 X-ray diffractometer (Shimadzu, Tokyo, Japan) 30 mA, 40 kV, $\lambda CuK\alpha$ = 0.15 nm with high diffraction angle 2θ varied from 0°–100° at the scan rate of 2°/min.

2.9 Atomic Force Microscope (AFM)

AFM is a high resolution microscope, through which microstructure of any material can be studied. AFM is an improvement to STM (Scanning Tunnelling Microscope), as in STM only conducting surfaces were analyzed whereas in AFM any and every material is fit to be used for microstructure investigation. Atomic Force Microscope (AFM) was carried on NT-MDT NEXT Solver (make-Russia) at Physics Laboratory of M.A.N.I.T, Bhopal. Here AFM is used for clear characterization of surface morphology like surface roughness and dispersion of GNPs nano particles in PU matrix.

3. RESULTS AND DISCUSSION

3.1 Uni-axial tensile, shape memory and shape fixity tests

Tensile strength of PU and composite having 1GPU samples were calculated from the Fig. 1 (by using Tinius Olsen 25kt tensile testing machine). The tensile strength and stiffness of composite were increases as compared to PU. Stiffness is defined as the area under the tensile graph. The region behind the increased tensile strength and stiffness was the embedded GNPs particles in the PU matrix. Another hand the moisture strongly influences the strength and stiffness of the

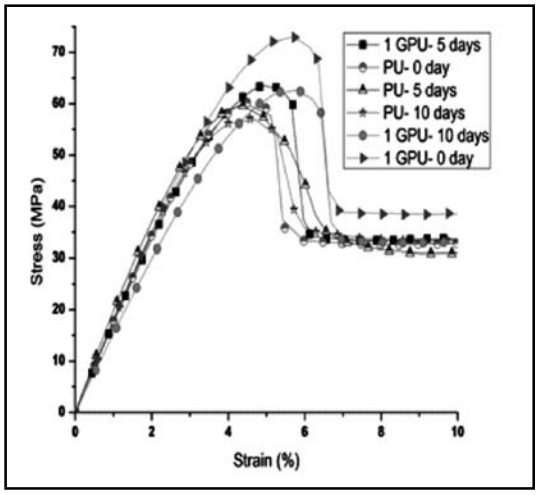

Fig. 1 Uniaxial Tensile stress-strain curves

samples. From Fig.1, it shows that tensile strength and stiffness of PU and composite were suppressed due to the moisture. As long as the water immersion days were increasing the strength goes to decreasing for both PU and 1 GPU samples. The maximum tensile strength 72 MPa was observed for 1 GPU without water immersion. And minimum tensile

strength for 1 GPU for 10 days water immersed sample was observed. Strength was suppressed due to the moisture because the absorbed water molecules react with the polymer chain and increase their chain mobility. Similar results also reported by many types of research [35-37]. When samples immersed in water for long days then the hydrogen bonding between the C=O and H-N groups is also weakened which is the main cause behind the decreased tensile strength and stiffness of moisture exposed samples.

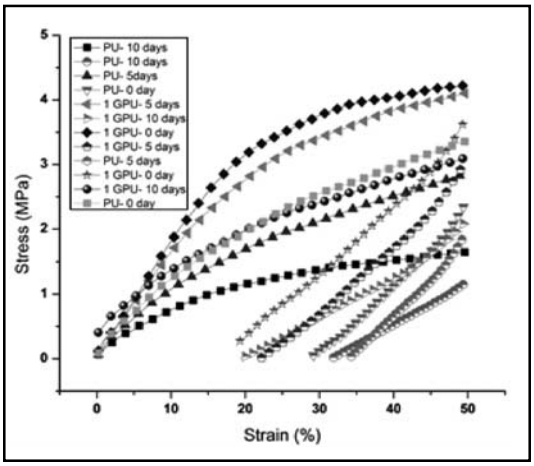

Fig. 2. Stretch and constrain recovery stress curves.

Fig. 2 shows that the shape memory stretch and constrain shape recovery strength of PU and 1 GPU samples by using the tensile testing machine with controlled temperature setup. For shape memory stretch and recovery tests, the procedure was similar as reported by [18, 38] which I have also explained in the experimental section. From Fig. 2 we concluded that with the addition of GNPs in PU matrix the stretch strength and constrain recovery strength both were significantly improved. Similar observations were also reported in a previous research paper [38]. Another hand the effect of moisture on shape memory stretch and recovery strength was strongly influenced. When the samples immersed in water for several days both stretch and recovery strength was decreased. From Fig. 2 it's observed that the maximum stretching strength for 1 GPU 0 day water immersion is 4 MPa and minimum stretching strength 1 MPa for PU 10 days water immersion. Also, the maximum recovery strength for 1 GPU is 3 MPa and minimum recovery strength 0.83 MPa for PU 10 days.

Shape fixity can be defined as the ability of the sample to maintain its temporary shape during cooling below its glass transition temperature. Mathematically it is expressed as the ration of fixed strain (ϵ_f) to the maximum deformed strain (ϵ_d).

$$R_f = \epsilon_f \div \epsilon_d \times 100$$

ϵ_f and ϵ_d were calculated as mentioned below;

$$\epsilon_f = (L_2 - L_0)/L \text{ and } \epsilon_d = (L_1 - L_0)/L_0$$

Where, L_0 is gauge length, L_1 maximum length after deforming and L_2 is the length of the specimen when load removed [18].

From Fig. 3 its clearly observed that with reinforcement of GNPs in PU matrix the shape fixity was improved. The improved shape fixity because the embedded GNPs in the PU matrix restrict the motion of soft segments which is responsible for shape recovery. For 1 GPU the shape fixity is almost 98 % and for PU it is 93 % only. Almost similar observations we also reported earliest [38]. From Fig. 3 we were also concluded that the shape fixity was drastically decreased due to the moisture samples.

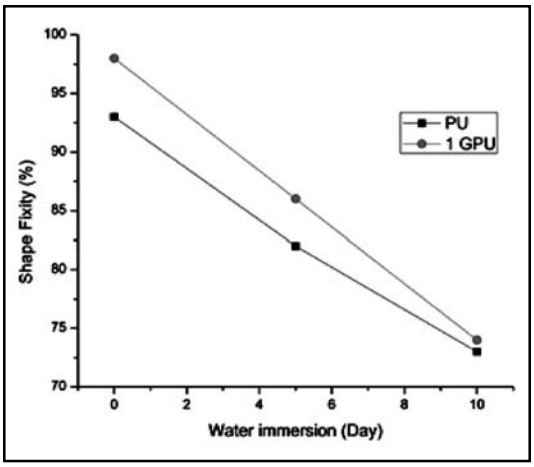

Fig. 3 Shape fixity curves.

Decrease shape fixity of water immersed samples because the molecules of water react with the PU chains and improve its chain mobility.

3.2 Surface morphology observation in Scanning Electron Microscopy (SEM)

Fig. 4 shows that the cryogenic fractured morphology of PU (Fig. 4 (a)) and 1 GPU (Fig. 4 (b)) by using the Scanning Electron Microscopy after gold coating for clear surface observations. From SEM Figure it clearly shows that the surface roughness was more in the composite sample as compared to the PU sample. The PU sample morphology is more smooth and uniform shape whereas for composite (1 GPU) it is rougher and randomly arranged. Randomly arranged morphology may conclude that the uniform distribution of GNPs in PU matrix which helps the superior properties. Researchers also reported the same results for composites and PU matrix [18, 38]

3.3 Dynamic Mechanical Analyser (DMA) tests:

The Dynamic Mechanical Analyser (DMA) was used for observation of thermo-mechanical properties of viscoelastic materials. The storage modulus (Fig. 5), loss modulus (Fig. 6) and energy dissipation factor (Fig.7) were calculated. And glass transition temperature also calculated by using DMA curves.

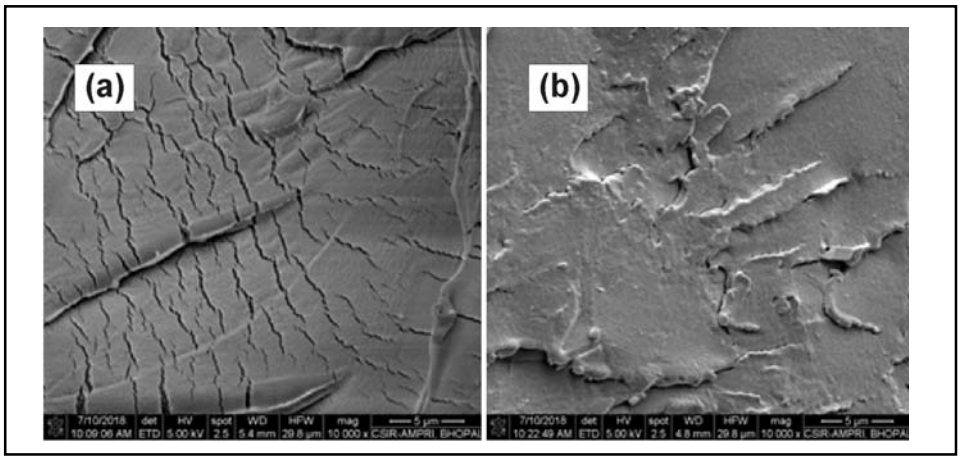

Fig. 4. Surface morphology (cryogenic fractured) (a) PU and (b) 1 GPU sample

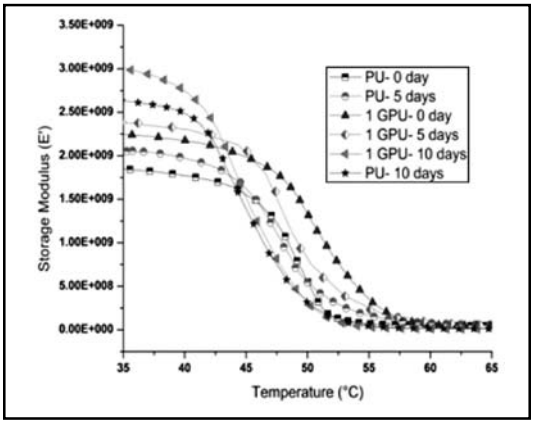

Fig. 5. Storage modulus curves.

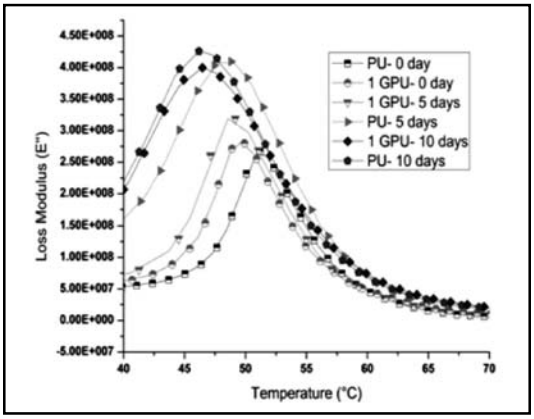

Fig. 6. Loss modulus curves.

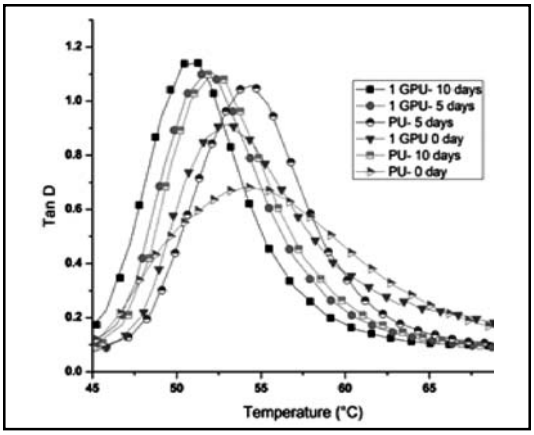

Fig. 7. Energy dissipation factor curves.

From Fig. 5 we can say that with the addition of GNPs in the PU matrix the elastic storage modulus was increased by 40 % for 1 GPU 0 day as compared to PU 0 day water immersion. Further, when the samples exposed in water the storage modulus was drastically increased for both PU and 1 GPU. The maximum storage modulus was observed for 1 GPU 10 days and minimum storage modulus for PU 0 day. And another hand the transition point shift toward the lower temperature which indicated that the glass transition temperature decreasing when samples exposed in moisture. Similar observations for glass transition temperature also observed in Fig. 6. Loss modulus may be defined as the stored energy converted into heat. The peaks of loss modulus curves shift toward the lower temperature for moisture samples. For 1 GPU 10 days and PU 10 days, water immersed sample loss modulus peaks is much closer to 40°C. The glass transition temperature near about 40°C (very closed to environments temperature) it may help for self-responsive shape memory polymer. Fig. 7 shows that the energy dissipation curves for PU and GPU. The energy dissipation factor is a ratio of loss modulus to the storage modulus. From Fig. 7 it's clear to observe that the peak of 1 GPU is higher than the PU sample which may indicate that the proper mixing and bonding between the GPs and the PU matrix. Another hand the peaks of water immersed samples were shifted towards the lower temperature. Shifted peaks toward lower temperature indicated that the loss of glass transition temperature. Details of glass transition temperature as shown in Table 1 by using DMA curves and DSC curves.

3.4 Differential Scanning Calorimetric (DSC):

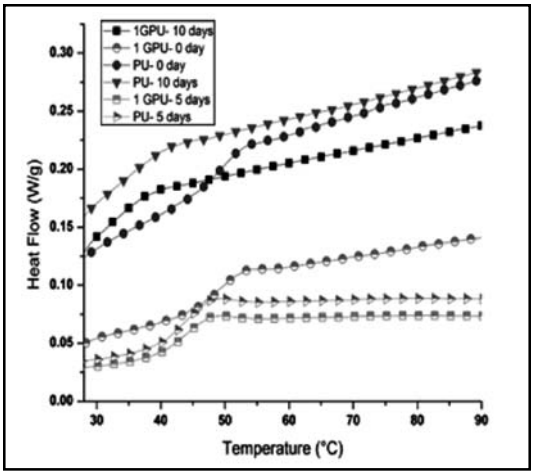

Fig. 8. DSC cooling curves

Differential Scanning Calorimetric (DSC) was used for calculation of glass transition temperature by using the half height. The DSC cooling curves shown in Fig. 8 for PU and 1 GPU were used for Tg calculation. Glass transition temperature is that temperature where the polymer changes its rubbery state to glassy state vice versa. From Fig. 8 we found that the glass transition temperature was decreased for 1 GPU as compared to the PU. Decreased glass transition temperate for 1 GPU composite because of the embedded GNPs in the PU matrix act as heat node which promotes the fast heating of the sample. And another hand the glass transition temperature also shifted toward the lower temperature when samples exposed in moisture. So that due to the moisture the glass transition temperature decreased. The many causes behind the decrease glass transition temperature one is the when water molecules react with the PU chains the hydrogen bonding between C=O and H-O groups weakened due to the moisture. Further, the amino and carbonyl groups interact with the water molecules and water molecules interact with the polymer chain and improve their mobility. Almost same experimental observation for moisture imposed thermoplastic polyurethane was reported by many researchers recently [36, 37].

TABLE 1. Calculation of glass transition temperature from DMA and DSC curves.

	PU 0 Day	**PU 5** Day	**PU 10** Day	**GPU 0** Day	**GPU 5** Day	**GPU 10** Day
Storage modulus curve	50°C	46°C	43°C	48°C	43°C	41°C
Loss modulus curve	57°C	51°C	46°C	55°C	48°C	46°C
Energy dissipation factor	56°C	53°C	49°C	54°C	49°C	47°C
DSC	55°C	48°C	40°C	53°C	46°C	38°C

3.5 MV-induced shape recovery tests

From Fig. 9 and Fig. 10 we concluded that the microwave-induced shape recovery tests for PU and 1 GPU samples. Fig. 9 shows that the MV-induced shape recovery of 1 GPU 0 day water immersed sample. It's clearly observed that the 1 GPU composite sample recover almost 100% original shape under MV irradiation within 20 seconds. For a composite sample, the embedded GNPs in the PU matrix

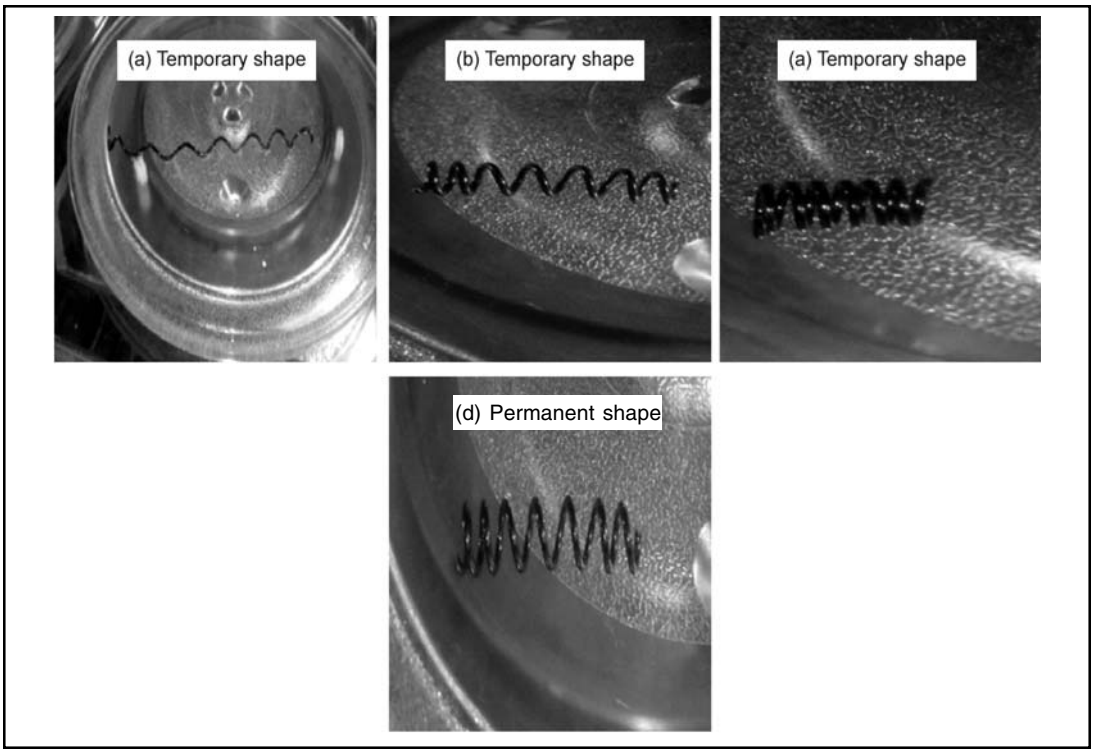

Fig. 9. MV-induced shape recovery exhibition of 1 GPU by using a digital camera (without water immersion)

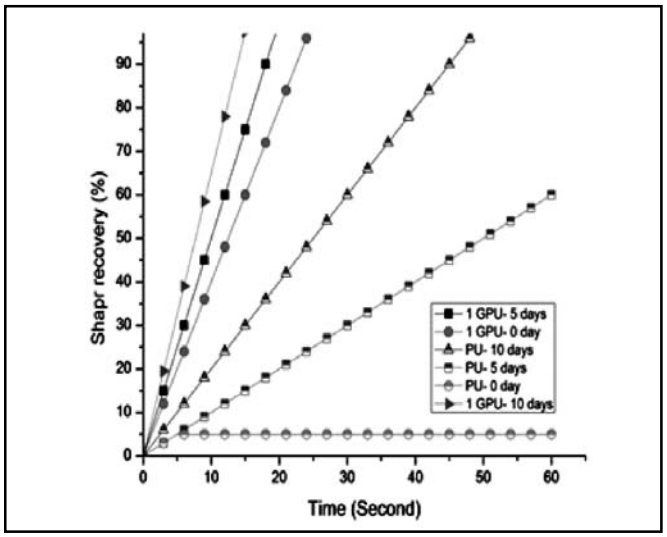

Fig. 10. Microwave-induced shape recovery of PU and 1 GPU samples tested in a microwave oven

act as a heat source under MV-irradiation which is responsible for fast shape recovery. Further, we try to discuss the effect of moisture on MV-induced shape recovery from Fig. 10. From MV shape recovery graph, the PU sample without exposing in moisture has no shape recovery during MV-irradiations (shown Fig. 10). Further when water immersed sample of PU was tested for MV-induced shape recovery than it's partially trying to recover original shape. The PU 10 days water immersed sample recovery its 90% original shape within 50 Seconds. Because the MV-irradiations absorbed by water molecules and PU water immersed sample got heated. Another hand the composite sample has also improved their shape recovery after water immersed for 10 days. So that we concluded that moisture (absorbed water molecules) act as a dielectric node, which absorbs the microwave and samples got heated, and samples recover its permanent shape.

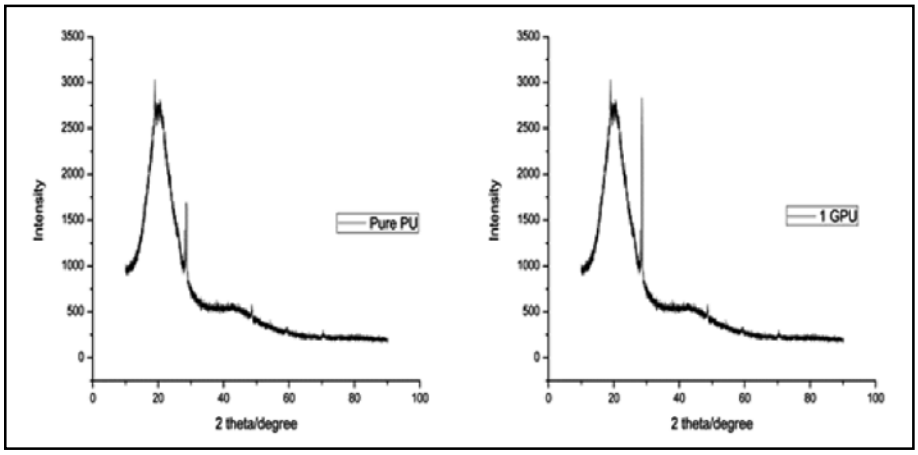

Fig. 11. XRD graphes of (a) polyurethane sample (Pure PU) (b) 1 GPU sample

X-Ray Diffraction (XRD) was used for examine the mixing characteristic of GNPs in polyurethane matrix. Fig. 11 shows that the XRD graphes of pure PU and composite containing 1 phr GNPs in PU matrix. the X-ray peaks of pure polyurethane shows in Fig. 11 (a), in PU two peaks shows near about 20° and 30°. The intensity of 20° peaks is higher than 30°, whereas in Fig. 11(b) shows 1GPU composite sample peaks. For 1 GPU sample the intensity of 30° peaks is higher as compared to PU sample. The increased intensity of peaks near about 30° indicated the proper mixing of GNPs in PU matrix because for graphene nanoplatelets peaks shown near 30°. Therefore we can say proper mixing may done during composite sample preparation because there is no peaks of graphitic in XRD pattern. Similar XRD observation was also reported by various eminent researchers [20, 27].

In this work Atomic Force Microscope (AFM) was carried out on NT-MDT NEXT Solver (make-Russia) at Physics Laboratory of M.A.N.I.T, Bhopal.

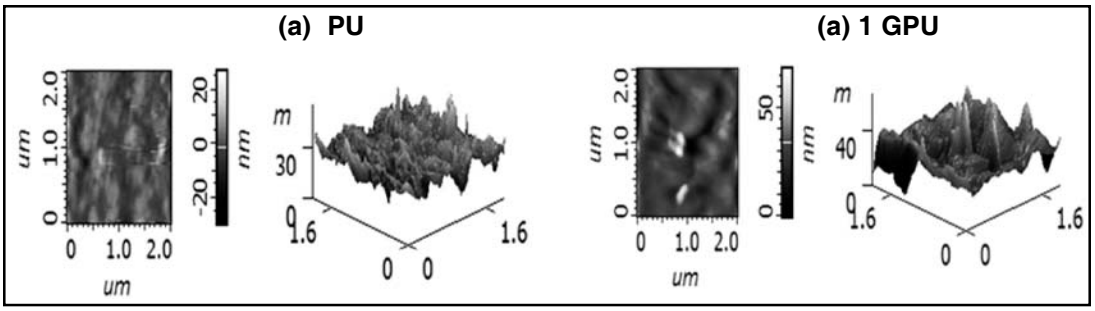

Fig. 12. AFM surface roughness of (a) PU and (b) 1GPU composite sample

The surface roughness of pure polyurethane and composite (1 GPU) containing 1 phr GNPs was studied by using AFM, which shows in Fig. 12. Fig. 12 (a) pure polyurethane shows that uniform surface roughness throughout the matrix and Fig. 12 (b) shows 1 GPU composite sample roughness and also distribution of graphene nanoplatelets in PU matrix. In composite sample the surface roughness is more random as compared to pure polyurethane matrix. The surface roughness of pure PU and 1 GPU matrix is around 30 nm and 45 nm respectively. Further, the waviness was also increased with the addition of GNPs in PU matrix. Random surface indicates the distribution of GNPs particles within the polyurethane matrix.

4. CONCLUSIONS

In present research work we concluded that the moisture plays an important role in shape memory and mechanical properties of MV-induced shape memory thermoplastic polyurethane/ graphene nanoplatelets (GNPs) composite. The properties like tensile strength, stretch and recovery strength, storage modulus, shape fixity, glass transition temperature were decreased due to the moisture, but shape recovery of specimens for PU and 1 GPU was increased. Amino and carbonyl groups of (PU) polymer chains interact with water molecules which improve the mobility of polymer chain. Further, the bonding between the C=O and H-N groups are weakened by the moisture which is responsible for inferior mechanical properties. The surface morphological (FE-SEM), XRD and AFM study shows that the proper mixing of GNPs in PU matrix which promotes the superior shape memory and mechanical properties. The PU sample has no shape recovery (MV-induced) without immersion in water but when the PU sample immersed in water it shows the MV-induced shape recovery. The reason behind these phenomena was the absorbed water molecules in PU act as a dielectric node which is the strong absorption of MV-irradiations.

The glass transition temperature was calculated by using the DMA curves and DSC curves; it shows that the transition temperature was continuously decreasing with increasing the water immersion days (moisture). The glass transition temperature (Tg) goes very close to 40°C when samples immersed in water for 10 days. The decreasing trend of glass transition temperature due to the moisture it may open the new gate for researchers to develop self-

shape recovery components or we can say moisture responsive shape memory polymer composite.

Acknowledgement

For this research work author great thank to National Institute of Technology Bhopal for providing the research grant and characterization facility. The author Krishan Kumar Patel also declare that “no conflict of interest”.

REFERENCES

1. Liu, C., H. Qin, and P. T. Mather. *Journal of materials chemistry* 17, no. 16 (2007): 1543-1558. DOI:10.1039/B615954K
2. Hager, Martin D., Stefan Bode, Christine Weber, and Ulrich S. Schubert. *Progress in Polymer Science* 49 (2015): 3-33.https://doi.org/10.1016/j.progpolymsci.2015.04.002
3. Pilate, Florence, Antoniya Toncheva, Philippe Dubois, and Jean-Marie Raquez. *European Polymer Journal* 80 (2016): 268-294.https://doi.org/10.1016/j.eurpolymj.2016.05.004
4. Castro, Francisco, Kristofer K. Westbrook, Jason Hermiller, Dae Up Ahn, Yifu Ding, and H. Jerry Qi. *Journal of Engineering Materials and Technology* 133, no. 2 (2011): 021025. doi:10.1115/1.4003103
5. Hu, Jinlian, Yong Zhu, Huahua Huang, and Jing Lu. *Progress in Polymer Science* 37, no. 12 (2012): 1720-1763. https://doi.org/10.1016/j.progpolymsci.2012.06.001
6. Han, Xiao Juan, Zhen Qiang Dong, Min Min Fan, Yan Liu, Jian Hu li, Yi Fu Wang, Qi Juan Yuan, Bang Jing Li, and Sheng Zhang. *Macromolecular rapid communications* 33, no. 12 (2012): 1055-1060. https://doi.org/10.1002/marc.201200153
7. Purohit, Rajesh, Krishan Kumar Patel, Gaurav Kumar Gupta, and R. S. Rana. *Materials Today: Proceedings* 4, no. 4 (2017): 5330-5335. https://doi.org/10.1016/j.matpr.2017.05.043
8. Westbrook, Kristofer K., Vikas Parakh, Taekwoong Chung, Patrick T. Mather, Logan C. Wan, Martin L. Dunn, and H. Jerry Qi. *Journal of Engineering Materials and Technology* 132, no. 4 (2010): 041010. doi:10.1115/1.4001964
9. Chen, Hongmei, Ying Li, Ye Liu, Tao Gong, Lin Wang, and Shaobing Zhou. *Polymer Chemistry* 5, no. 17 (2014): 5168-5174. DOI: 10.1039/C4PY00474D
10. Liu, Yiping, Ken Gall, Martin L. Dunn, and Patrick McCluskey. *Mechanics of Materials* 36, no. 10 (2004): 929-940. https://doi.org/10.1016/j.mechmat.2003.08.012
11. Yang, B., W. M. Huang, C. Li, and L. Li. *Polymer* 47, no. 4 (2006): 1348-1356. https://doi.org/10.1016/j.polymer.2005.12.051
12. Meng, Harper, and Guoqiang Li. *Polymer* 54, no. 9 (2013): 2199-2221. https://doi.org/10.1016/j.polymer.2013.02.023
13. Du, Haiyan, Zhen Song, Jingjing Wang, Zhenhai Liang, Yinghua Shen, and Feng You. *Sensors and Actuators A: Physical* 228 (2015): 1-8. https://doi.org/10.1016/j.sna.2015.01.012
14. Du, Haiyan, Yunlong Yu, Guangming Jiang, Junhua Zhang, and JianJun Bao. *Macromolecular Chemistry and Physics* 212, no. 14 (2011): 1460-1468. https://doi.org/10.1002/macp.201100149
15. Cao, Feina, and Sadhan C. Jana. *Polymer* 48, no. 13 (2007): 3790-3800. https://doi.org/10.1016/j.polymer.2007.04.027
16. Park, Jin Ho, Trung Dung Dao, Hyung-il Lee, Han Mo Jeong, and Byung Kyu Kim. *Materials* 7, no. 3 (2014): 1520-1538. DOI:10.3390/ma7031520
17. Ponnamma, Deepalekshmi, Kishor Kumar Sadasivuni, Michael Strankowski, Paula Moldenaers, Sabu Thomas, and Yves Grohens. *Rsc Advances* 3, no. 36 (2013): 16068-16079. DOI: 10.1039/C3RA41395K
18. Hashmi, S. A. R., Harish Chandra Prasad, R. Abishera, Hari Narayan Bhargaw, and Ajay Naik. *Materials & Design* 67 (2015): 492-500. https://

doi.org/10.1016/j.matdes.2014.10.062

19. Choi, Jin Taek, Trung Dung Dao, Kyung Min Oh, Hyung-il Lee, Han Mo Jeong, and Byung Kyu Kim. *Smart Materials and Structures* 21, no. 7 (2012): 075017. .https://doi.org/10.1088/0964-1726/21/7/075017

20. Shimamoto, Akira, Jai-Sug Hawong, and Hyo-Jae Lee. *Journal of engineering materials and technology* 124, no. 4 (2002): 390-396. DOI: 10.1115/1.1494449

21. Park, Jin Ho, Trung Dung Dao, Hyung-il Lee, Han Mo Jeong, and Byung Kyu Kim. *Materials* 7, no. 3 (2014): 1520-1538. doi:10.3390/ma7031520

22. Liu, C., H. Qin, and P. T. Mather. *Journal of materials chemistry* 17, no. 16 (2007): 1543-1558. DOI: 10.1039/B615954K

23. Liang, Jiajie, Yanfei Xu, Yi Huang, Long Zhang, Yan Wang, Yanfeng Ma, Feifei Li, Tianying Guo, and Yongsheng Chen. *The Journal of Physical Chemistry C* 113, no. 22 (2009): 9921-9927.DOI: 10.1021/jp901284d

24. Kausar, Ayesha, and Amin Ur Rahman. *Fullerenes, Nanotubes and Carbon Nanostructures* 24, no. 4 (2016): 235-242. https://doi.org/10.1080/1536383X.2016.1144592

25. Liu, Xuefa, Hua Li, Qingping Zeng, Yangyang Zhang, Hongmei Kang, Huanan Duan, Yiping Guo, and Hezhou Liu. *Journal of Materials Chemistry A* 3, no. 21 (2015): 11641-11649. DOI:10.1039/C5TA02490K

26. Liu, Yanju, Haibao Lv, Xin Lan, Jinsong Leng, and Shanyi Du. *Composites Science and Technology* 69, no. 13 (2009): 2064-2068. https://doi.org/10.1016/j.compscitech.2008.08.016

27. Invernizzi, Marta, Stefano Turri, Marinella Levi, and Raffaella Suriano. *European Polymer Journal* 101 (2018): 169-176. https://doi.org/10.1016/j.eurpolymj.2018.02.023

28. Song, Janice J., Huntley H. Chang, and Hani E. Naguib. *European Polymer Journal* 67 (2015): 186-198. https://doi.org/10.1016/j.eurpolymj.2015.03.067

29. Yu, Li, and Haifeng Yu. *ACS applied materials & interfaces* 7, no. 6 (2015): 3834-3839. **DOI:** 10.1021/am508970k

30. Yu, Li, Zhangxiang Cheng, Zhijiao Dong, Yihe Zhang, and Haifeng Yu. *Journal of Materials Chemistry C* 2, no. 40 (2014): 8501-8506. DOI: 10.1039/C4TC01097C

31. Nag, Anindya, Arkadeep Mitra, and Subhas Chandra Mukhopadhyay. *Sensors and Actuators A: Physical* 270 (2018): 177-194. ttps://doi.org/10.1016/j.sna.2017.12.028

32. Quan, Maohua, Bowen Yang, Jingxia Wang, Haifeng Yu, and Xinyu Cao. *ACS applied materials & interfaces* 10, no. 4 (2018): 4243-4249. **DOI:** 10.1021/acsami.7b17230

33. Cheng, Zhangxiang, Tianjie Wang, Xiao Li, Yihe Zhang, and Haifeng Yu. *ACS applied materials & interfaces* 7, no. 49 (2015): 27494-27501. **DOI:** 10.1021/acsami.5b09676

34. Huang, W. M., B. Yang, L. An, C. Li, and Y. S. Chan. *Applied Physics Letters* 86, no. 11 (2005): 114105. https://doi.org/10.1063/1.1880448

35. Yang, B., W. M. Huang, C. Li, C. M. Lee, and L. Li. *Smart materials and structures* 13, no. 1 (2003): 191..https://doi.org/10.1088/0964-1726/13/1/022

36. Yang, Bin, Wei Min Huang, Chuan Li, and Jun Hoe Chor. *European Polymer Journal* 41, no. 5 (2005): 1123-1128. https://doi.org/10.1016/j.eurpolymj.2004.11.029

37. Huang, W. M., B. Yang, Y. Zhao, and Z. Ding. *Journal of materials chemistry* 20, no. 17 (2010): 3367-3381. DOI:10.1039/B922943D

38. Patel, Krishan Kumar, and Rajesh Purohit. *Sensors and Actuators A: Physical* 285 (2019): 17-24. https://doi.org/10.1016/j.sna.2018.10.049

39. Patel, Krishan Kumar, and Rajesh Purohit. *Materials Today: Proceedings* 5, no. 9 (2018): 20193-20200. https://doi.org/10.1016/j.matpr. 2018.06.389

40. Belmonte, Alberto, Giuseppe C. Lama, Gennaro Gentile, Pierfrancesco Cerruti, Veronica Ambrogi, Xavier Fernández-Francos, and Silvia De la Flor.

European Polymer Journal 97 (2017): 241-252. https://doi.org/10.1016/j.eurpolymj.2017.10.006

41. Gu, Shuying, Beibei Yan, Lingling Liu, and Jie Ren. *European Polymer Journal* 49, no. 12 (2013): 3867-3877. https://doi.org/10.1016/j.eurpolymj.2013.10.007

42. Zhou, Liming, Qiang Liu, Xuande Lv, Lijun Gao, Shaoming Fang, and Haifeng Yu. *Journal of Materials Chemistry C* 4, no. 42 (2016): 9993-9997. DOI: 10.1039/C6TC03556F

43. Yu, Kai, Yanju Liu, and Jinsong Leng. *Rsc Advances* 4, no. 6 (2014): 2961-2968. DOI: 10.1039/C3RA43258K

44. Senatov, F. S., M. Yu Zadorozhnyy, K. V. Niaza, V. V. Medvedev, S. D. Kaloshkin, N. Yu Anisimova, M. V. Kiselevskiy, and Kai-Chiang Yang. *European Polymer Journal* 93 (2017): 222-231. https://doi.org/10.1016/j.eurpolymj.2017.06.011

Received: 12-01-2019

Accepted: 31-01-2019